Makris, N. & Gazetas, G. (1993). *Géotechnique* **43**, No. 1, 135–150

Displacement phase differences in a harmonically oscillating pile

N. MAKRIS* and G. GAZETAS*

Analytical solutions are developed for harmonic wave propagation in an axially or laterally oscillating pile embedded in homogeneous soil and excited at the top. Pile–soil interaction is realistically represented through a dynamic Winkler model, the springs and dashpots of which are given values based on results of finite element analyses with the soil treated as a linear hysteretic continuum. Closed form expressions are derived for the phase velocities of the generated waves; these are compared with characteristic phase velocities in rods and beams subjected to compression–extension (axial) and flexural (lateral) vibrations. The role of radiation and material damping is elucidated; it is shown that the presence of such damping radically changes the nature of wave propagation, especially in lateral oscillations where an upward propagating (reflected) wave is generated even in a semi-infinite head-loaded pile. Solutions are then developed for the phase differences between pile displacements at various depths. For most piles such differences are not significant and waves emanate nearly simultaneously from the periphery of an oscillating pile. This conclusion is useful in analysing dynamic pile to pile interaction, the consequences of which are shown in this Paper.

KEYWORDS: deformation; dynamics; piles; vibration; waves.

Des solutions analytiques ont été développées afin d'étudier la propagation harmonique des ondes dans un pieu ancré dans un sol homogène, excité à son sommet, et oscillant latéralement et axialement. L'interaction sol-pieu est bien représentée par le modèle dynamique de Winkler dont les ressorts et 'pistons' sont affectés de valeurs calculées à partir d'analyses par éléments finis, le sol étant supposé à hystérésis linéaire. Des expressions de forme équivalente sont dérivées pour calculer les vitesses de phase des ondes induites. Elles sont comparées aux vitesses en phase caractéristiques obtenues dans des barres et poutres soumises à des vibrations de type compression-extension (axiales) ou de type flexion (latérales). Le rôle de la radiation et celui du 'damping' du matériau sont expliqués; l'on montre que l'existence d'un 'damping' modifie totalement la nature de la propagation des ondes, tout particulièrement lors d'oscillations latérales où une onde se propageant vers le haut apparaît, même dans un pieu semi-infini chargé à son sommet. Des solutions permettant de calculer les différences de phase entre les déplacements des pieux à différentes profondeurs sont alors développées. Pour la plupart des pieux, ces différences ne sont pas significatives et les ondes émergent à peu près simultanément de la périphérie du pieu oscillant. Cette conclusion est très utile pour l'analyse de l'interaction dynamique pieu-pieu dont l'article décrite les conséquences.

INTRODUCTION

This work was prompted by the need to develop a deeper understanding of some of the wave propagation phenomena associated with the dynamic response of piles and pile groups. For example, it is well known (Kaynia & Kausel, 1982; Nogami, 1983; Novak, 1985; Roesset, 1984) that two neighbouring piles in a group may affect each other so substantially that the overall dynamic behaviour of the group is vastly different from that of each individual pile. This pile to pile interaction is frequency-dependent and is a consequence of waves that are emitted from the periphery of each pile and propagate until they 'strike' the other pile.

As an example, for a square group of 2×2 rigidly-capped piles embedded in a deep homogeneous stratum Fig. 1 shows the variation with frequency of the vertical and horizontal dynamic group stiffness and damping factors, defined as the ratios of the group dynamic stiffness and dashpot coefficients, respectively, to the sum of the static stiffnesses of the individual solitary piles. At zero frequency the stiffness group factors reduce to the respective static group factors (also called 'efficiency factors' by geotechnical engineers) which are invariably smaller than unity.

The continuous curves in Fig. 1, adopted from the rigorous solution of Kaynia & Kausel (1982), reveal that, as a result of dynamic pile to pile

Discussion on this Paper closes 1 July 1993; for further details see p. ii.

* State University of New York at Buffalo and National Technical University of Athens.

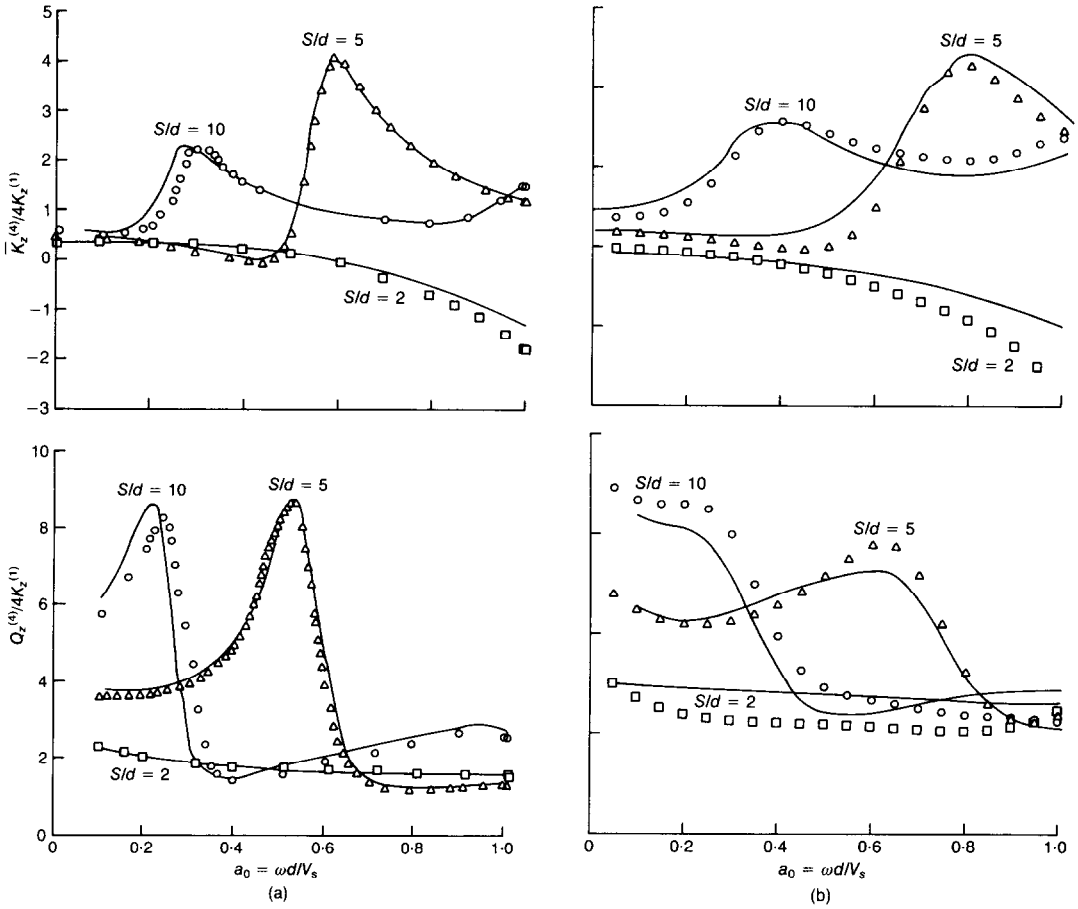

Fig. 1. Normalized vertical and lateral impedances of a 2 × 2 pile group ($E_p/E_s = 1000$, $L/d = 15$, $\nu = 0{\cdot}4$, $\beta = 0{\cdot}05$): solid curves = rigorous solution of Kaynia & Kausel (1982); points = simplified solution of : (a) Dobry & Gazetas (1988); (b) Makris & Gazetas (1992) (impedances are expressed as $\bar{K} + ia_0 Q$; subscripts z and x refer to vertical and horizontal mode; $\bar{K}^{(4)}$ and $Q^{(4)}$ are the total dynamic stiffness and damping of the 4-pile group; $K^{(1)}$ is the static stiffness of the single (solitary) pile)

interaction, the dynamic stiffness group factors achieve values that may far exceed the static efficiency factors, and may even exceed unity. Both stiffness and damping factors are not observed in the single pile response. Specifically, the peaks of the curves occur whenever waves originating with a certain phase from one pile arrive at the adjacent pile in exactly opposite phase, thereby inducing an upwards displacement at a moment when the displacement due to this pile's own load is downwards. Thus, a larger force must be applied to this pile to enforce a certain displacement amplitude, resulting in a larger overall stiffness of the group as compared to the sum of the individual pile stiffnesses.

Also shown in Fig. 1 as points are the results of a very simple analytical method of solution proposed by Dobry & Gazetas (1988) and further developed by Makris & Gazetas (1992), Makris, Gazetas & Fan (1992) and Gazetas & Makris (1991). The method introduces a number of physically motivated approximations, and was originally intended merely to provide a simple engineering explanation of the causes of the numerically observed peaks and troughs in the dynamic impedances of pile groups. Yet, as is evident from the comparisons shown in Fig. 1, the results of the method plot remarkably close to the rigorous curves for all three pile separation distances considered (two, five and ten pile diameters). Even some detailed trends in the group response seem to be adequately captured by the simple solution. Further successful comparisons are given in the above-mentioned references.

The fundamental idea of this method is that the

displacement field created along the sidewall of an oscillating pile (in any mode of vibration) propagates and affects the response of neighbouring piles. It is assumed that cylindrical waves are emitted from the perimeter of an oscillating pile, and propagate horizontally in the r direction only. This hypothesis is reminiscent of the shearing concentric cylinders around statically loaded pile and pile groups assumed by Randolph & Wroth (1978, 1979), and is also similar to the dynamic Winkler assumption introduced by Novak (1974) and extensively used with success in dynamic analyses of pile groups. It is further assumed that these cylindrical waves emanate simultaneously from all points along the pile length; hence for a homogeneous deposit they spread out in phase and form a cylindrical wavefront, concentric with the generating pile (unless the pile is rigid, the amplitude of oscillation along the wavefront will be a (usually decreasing) function of depth). The resulting dynamic complex-valued pile to pile interaction factor for vertical oscillation takes the simple form (Dobry & Gazetas, 1988)

$$\alpha_v = \left(\frac{r_0}{S}\right)^{1/2} \exp\left(-\beta\omega \frac{S}{V_s}\right) \exp\left(-i\omega \frac{S}{V_s}\right) \quad (1)$$

where $r_0 = d/2$ is the radius of the pile, S is the axis to axis distance of the piles, and V_s and β are the S wave velocity and hysteretic damping ratio of the soil respectively.

The most crucial of the introduced simplifying assumptions is that the waves created by an oscillating pile emanate simultaneously from all perimetric points along the pile length, and hence, for a homogeneous stratum, form cylindrically expanding waves that would 'strike' an adjacent pile simultaneously at various points along its length, i.e. the arriving waves are all in phase, although their amplitudes decrease with depth.

The question arises as to whether the satisfactory performance of such a simple method is merely a coincidence (e.g. due to cancellation of errors), or a consequence of fundamentally sound physical approximations. Answering this question was one of the motives for the work reported in this Paper. Hence, the first objective was to investigate whether or not this key assumption of synchronous wave emission from an oscillating pile is indeed a reasonable engineering approximation and, if it is, for what ranges of problem parameters.

A second, broader, objective of the Paper is to obtain a deeper physical insight into the nature of wave propagation in a single harmonically oscillating pile embedded in homogeneous soil. To this end, realistic dynamic Winkler-type models for vertically and horizontally oscillating single piles are developed, from which analytical solutions are derived for the apparent phase velocities of the waves propagating along the pile and for the variation with depth of pile displacements and phase angle differences. A limited number of rigorous finite element results are also obtained to substantiate the findings of the Winkler model. It is shown that the apparent phase velocities for typical piles are indeed quite large, and the displacement phase differences correspondingly small, especially within the upper, most active part of the pile. It is also found that at very high frequencies the phase velocities in a pile embedded in homogeneous soil become asymptotically equal to the wave velocities of an unsupported bar or beam in longitudinal and flexural oscillations.

PROBLEM DEFINITION

The problem studied involves a single floating pile embedded in a uniform halfspace and subjected at its head to a harmonic loading of circular frequency ω. The pile is a linearly elastic flexural beam of Young's modulus E_p, diameter d, cross-sectional area A_p, bending moment of inertia I_p and mass per unit length m. The soil is modelled as dynamic Winkler medium, resisting pile displacements through continuously distributed linear springs (k_x or k_z) and dashpots (c_x or c_z), as shown in Fig. 2 for horizontal (x) and vertical (z) motion. For the problem of lateral vibration (horizontal motion), the pile is considered to be fixed-head (zero rotation at the top). The force to displacement ratio of the Winkler medium at every depth defines the complex-valued impedances $k_z + i\omega c_z$ (vertical motion) or $k_x + i\omega c_x$ (horizontal motion), $i = \sqrt{(-1)}$, where c_z and c_x would, in general, reflect both radiation and material damping in the soil. k_z and k_x are in units of stiffness per unit length of the pile (i.e. $[F]\,[L]^{-2}$); they correspond to the traditional subgrade modulus (in units $[F]\,[L]^{-3}$) multiplied by the width (diameter) d of the pile.

Frequency-dependent values are assigned to these uniformly-distributed spring and dashpot coefficients, using the following algebraic expressions developed by matching the dynamic pile-head displacement from Winkler and from dynamic finite-element analyses (Roesset & Angelides, 1979; Blaney, Kausel & Roesset, 1976; Dobry *et al.*, 1982; Gazetas & Dobry, 1984a, 1984b)

$$k_z \approx 0{\cdot}6E_s(1 + \tfrac{1}{2}\sqrt{a_0}) \quad (2a)$$

$$c_z \approx (c_z)_{\text{radiation}} + (c_z)_{\text{hysteresis}}$$

$$\approx 1{\cdot}2a_0^{-1/4}\pi d\rho_s V_s + 2\beta \frac{k_z}{\omega} \quad (2b)$$

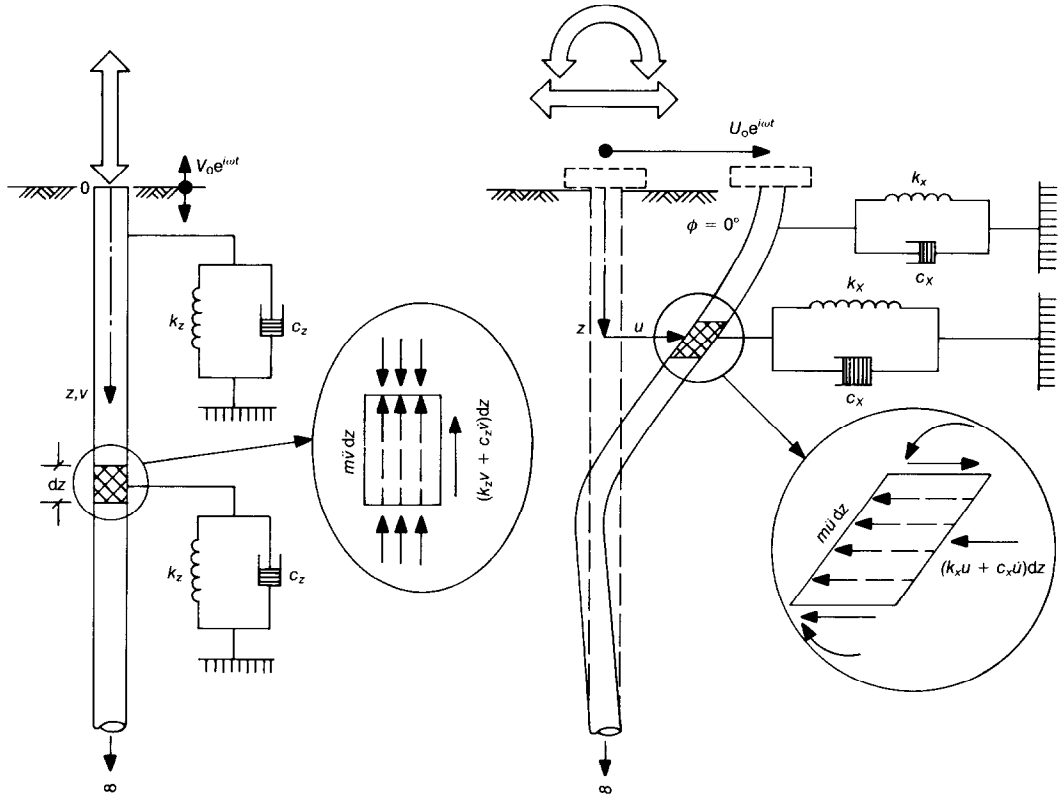

Fig. 2. Dynamic Winkler model for axially and laterally oscillating pile

$$k_x \approx 1{\cdot}2E_s \tag{2c}$$

$$c_x \approx (c_x)_{\text{radiation}} + (c_x)_{\text{hysteresis}}$$

$$\approx 2d\rho V_s\left[1 + \left(\frac{V_{La}}{V_s}\right)^{5/4}\right]a_0^{-1/4} + 2\beta\frac{k_x}{\omega} \tag{2d}$$

where β is hysteretic damping, ρ_s is mass density, E_s is Young's modulus, V_s is S-wave velocity of the soil, $a_0 = \omega d/V_s$ and V_{La} is an apparent velocity of the compression–extension waves, called 'Lysmer's analogue' velocity (Gazetas & Dobry, 1984a, 1984b)

$$V_{La} = \frac{3{\cdot}4}{\pi(1-\nu)V_s} \tag{3}$$

where ν is the Poisson's ratio of the soil. For an average typical value $\nu = 0{\cdot}4$, equation (3) gives $V_{La} \approx 1{\cdot}8V_s$ and equation (2d) simplifies to

$$c_x \approx 6a_0^{-1/4}d\rho V_s + 2\beta\frac{k_x}{\omega} \tag{4}$$

Similar springs and dashpots can be obtained using Novak's plane-strain elastodynamic solution for a rod oscillating in a continuum (Novak, 1974, 1977, 1985; Novak *et al.*, 1978). Novak's results would be exact for an infinitely long, infinitely rigid rod fully embedded in a continuum space. In contrast, equations (2b) and (2d) for radiation damping are derived in two steps

(*a*) their form is determined from a simple one-dimensional 'cone' model (Gazetas & Dobry, 1984a; Gazetas, 1987; Wolf, 1992) which resembles Novak's model but does allow for some non-zero vertical deformation of the soil during lateral motion, as is appropriate due to the presence of the stress-free surface and to the non-uniformity with depth of pile deflexions

(*b*) the numerical coefficients of the two expressions are then calibrated by essentially curve-fitting rigorous finite element results for a variety of pile–soil geometries and properties, as well as for different loading conditions (Gazetas & Dobry, 1984a; Gazetas, 1987; Wolf, 1992).

The spring constants, however, are derived solely through curve-fitting, i.e. by matching pile-head stiffnesses of the Winkler and the finite

element formulations. One approximation introduced in deriving equations (2a–2d) is to neglect the (relatively small) influence of pile slenderness and flexibility (measured for example through L/d and E_p/E_s).

The resulting values from equations (2)–(4) for k_z, c_z, k_x and c_x at various frequencies are generally comparable with those of Novak. Equations (2)–(4) are preferred for three reasons: first, they are simpler (as they do not involve complicated expressions with Bessel functions of complex argument). Second, they avoid the substantial underestimation of stiffness values by the plane-strain model at frequencies $\omega d/V_s < 1$, i.e. in the range of practical interest. (Novak compensates for this underestimation through a simple intuitive adjustment, which assumes constant k_z and k_x below two different 'cut-off' frequencies.) Third, the lateral radiation damping expression of equation (2d) does not show the spurious high sensitivity to Poisson's ratio observed in the plane-strain Novak's solution, which arises mainly from the unrealistic restriction of vertical soil deformation.

It is also worth noting that dynamic Winkler springs and dashpots have been derived by Liou & Penzien (1980), Roesset & Angelides (1980) and Kagawa & Kraft (1980), using yet another methodology. They all used three-dimensional formulations (based on either Midlin's static solution or finite element modelling) to relate local unit soil reaction to local pile deflexion at various depths along the pile; a single complex-valued dynamic stiffness S_z and S_x to be uniformly distributed as springs and dashpots along the pile (as is appropriate for a Winkler foundation) was then derived by a suitable integration of local stiffnesses over depth. Only a small number of results, pertaining to a uniform soil stratum, have been presented in those studies.

All these alternative methods give k and c values that are in reasonable agreement for the range of frequencies of greatest interest ($a_0 < 1$): individual differences in the Winkler parameters do not exceed 10–20%. The findings of this Paper can be shown to be quite insensitive to such differences; hence any set of expressions for the Winkler parameters could have been adopted successfully.

The c_x values obtained from equations (2c), (2d) and (4) apply in real situations only for frequencies ω above the stratum cutoff frequency ω_{cutoff}. The latter is nearly identical to the natural frequency $\omega_s = (\pi/2)V_s/H$ in horizontal (shear) vibrations of the soil stratum. For $\omega < \omega_s$ radiation damping is vanishingly small, in function of the material damping; it may then be stated that

$$c_x \approx (c_x)_{\text{hysteresis}} = 2\beta k_x/\omega \tag{5}$$

Similarly, the c_z expression in equations (2a) and (2b) applies only for frequencies above the stratum cutoff frequency in vertical compression–extension vibration, which is approximately equal to

$$\omega_c \approx 3{\cdot}4\omega_s/[\pi(1-\nu)] \tag{6}$$

For $\omega < \omega_c$

$$c_z \approx (c_z)_{\text{hysteresis}} = 2\beta k_z/\omega \tag{7}$$

AXIAL VIBRATION

Governing equations and solution

For very short (say, $L/d < 10$) and stiff ($E_p/E_s > 8000$) piles, the basic validity of the simplifying assumption of synchronous wave emission is self-evident, as such piles respond essentially as rigid bodies to axial loading (static or dynamic). For the other extreme case, of long and flexible piles, the pile is considered here as an infinite elastic 'thin' rod (i.e. lateral inertia effects are ignored, in accordance with classical rod theory). The deflected state of such a pile and the forces acting on an element are shown in Fig. 2. For harmonic steady-state oscillations, the vertical displacement $v(z, t)$ of a point on a cross-section of the pile at depth z and time t can be written as

$$v(z, t) = v(z)\, e^{i\omega t} \tag{8}$$

and dynamic equilibrium yields

$$E_p A_p \frac{d^2v(z)}{dz^2} - (k_z + i\omega c_z - m\omega^2)v(z) = 0 \tag{9}$$

Solutions are obtained separately for each of the two possible cases $\omega < \bar{\omega}_z$ and $\omega \geq \bar{\omega}_z$, where

$$\bar{\omega}_z = (k_z/m)^{1/2} \tag{10}$$

First, consider $\omega < \bar{\omega}_z$. This inequality translates approximately to $a_0 < 1{\cdot}8$, which is the usual range of practical interest in foundation problems. Equation (9) can be written as

$$\frac{d^2v(z)}{dz^2} - \lambda^2 v(z) = 0 \tag{11}$$

where λ^2 is a complex number (having positive real and imaginary parts) with

$$\lambda = R\left(\cos\frac{\theta}{2} + i\sin\frac{\theta}{2}\right) \tag{12}$$

where

$$R = \left[\frac{(k_z - m\omega^2)^2 + (\omega c_z)^2}{(E_p A_p)^2}\right]^{1/4} \tag{13}$$

$$\theta = \tan^{-1}\left(\frac{\omega c_z}{k_z - m\omega^2}\right), \quad 0 < \theta < \frac{\pi}{2} \tag{14}$$

The solution to equation (11) is

$$v(z, t) = A_1 \exp\left(R \cos\frac{\theta}{2} z\right) \times \exp\left[i\left(\omega t + R \sin\frac{\theta}{2} z\right)\right] + A_2 \exp\left(-R \cos\frac{\theta}{2} z\right) \times \exp\left[i\left(\omega t - R \sin\frac{\theta}{2} z\right)\right] \quad (15)$$

where A_1 and A_2 are integration constants to be determined from the boundary conditions. For the displacement to remain finite as z tends to infinity, A_1 must vanish. If V_0 is the displacement at the pile head ($z = 0$), equation (15) leads to

$$v(z, t) = V_0 \exp\left(-R \cos\frac{\theta}{2} z\right) \times \exp\left[i\left(\omega t - R \sin\frac{\theta}{2} z\right)\right] \quad (16)$$

For an applied harmonic load $P_0 \exp(i\omega t)$ at the top of the pile (P_0 is a real number), the pile-head displacement is a complex number (its real part being the component that is in phase with the applied force, while the imaginary part is the out-of-phase component)

$$V_0 = \frac{P_0\left(\cos\frac{\theta}{2} - i \sin\frac{\theta}{2}\right)}{RE_p A_p} \quad (17)$$

where R and θ are given by equations (13) and (14) respectively. It can be checked that when $\omega = 0$ (i.e. under static loading), $\theta = 0$ and equation (14) reduces to the familiar static expression (Roesset & Angelides, 1980)

$$V_0 = \frac{P_0}{\sqrt{(k_z E_p A_p)}} \quad (18)$$

Equation (16) represents a travelling wave of amplitude decreasing exponentially with depth and of phase velocity

$$C_a = \frac{\omega}{R \sin \theta/2} \quad (19)$$

in which both R and θ are functions of the frequency ω, and depend on the damping c_z. With an arbitrary dynamic loading, when several frequencies would be present, each harmonic component of motion would propagate with a different velocity, and therefore the motion experienced by a receiver at a neighbouring location would be different (less pronounced) than the input (source) motion: hence the term 'dispersion' relation which is used in wave propagation theory to describe such an equation.

Second, consider $\omega \geq \bar{\omega}_z$. This inequality translates to approximately $a_0 > 1{\cdot}8$, a frequency range of lesser interest, but nevertheless examined here as it gives an insight into asymptotic behaviour at high frequencies. The solution now takes the form

$$v(z, t) = V_0 \exp\left(R \sin\frac{\theta}{2} z\right) \times \exp\left[i\left(\omega t - R \cos\frac{\theta}{2} z\right)\right] \quad (20)$$

where R is as in equation (13), but θ is negative ($-\pi/2 < \theta < 0$).

In this case

$$V_0 = \frac{-P_0\left(\sin\frac{\theta}{2} + i \cos\frac{\theta}{2}\right)}{RE_p A_p} \quad (21)$$

Equation (20) represents a travelling wave with amplitude decreasing exponentially with depth and a phase velocity

$$C_a = \frac{\omega}{R \cos \theta/2} \quad (22)$$

Equation (22) is the dispersion relation for the second case.

Discussion of results

From the dispersion relation of equation (19), the ratio of the pile phase velocity to the soil S-wave velocity is obtained

$$\frac{C_a}{V_s} = \frac{a_0\sqrt{[(\pi/4)s_2]}}{\{[f_1 - (\pi/4)s_1 s_3 a_0{}^2]^2 + f_2{}^2\}^{1/2} \times \sin\{\tfrac{1}{2}\tan^{-1}[f_2/(f_1 - (\pi/4)s_1 s_3 a_0{}^2)]\}} \quad (23)$$

where

$$s_1 = G_s/E_s \quad (24a)$$

$$s_2 = E_p/E_s \quad (24b)$$

$$s_3 = \rho_p/\rho_s \quad (24c)$$

$$f_1 = 0{\cdot}6(1 + 0{\cdot}5\sqrt{a_0}) \quad (24d)$$

$$f_2 = 1{\cdot}2\pi s_1 a_0^{3/4} + 2\beta f_1 \quad (24e)$$

The ratio C_a/V_s is plotted against a_0 in Fig. 3 for two characteristic values of relative pile stiffness, $s_2 = E_p/E_s = 1000$ and 5000, and two pile mass densities, $\rho_p = 0{\cdot}7\rho_s$ and $1{\cdot}4\rho_s$. In the frequency range of greatest practical interest (i.e. for $0{\cdot}2 <$

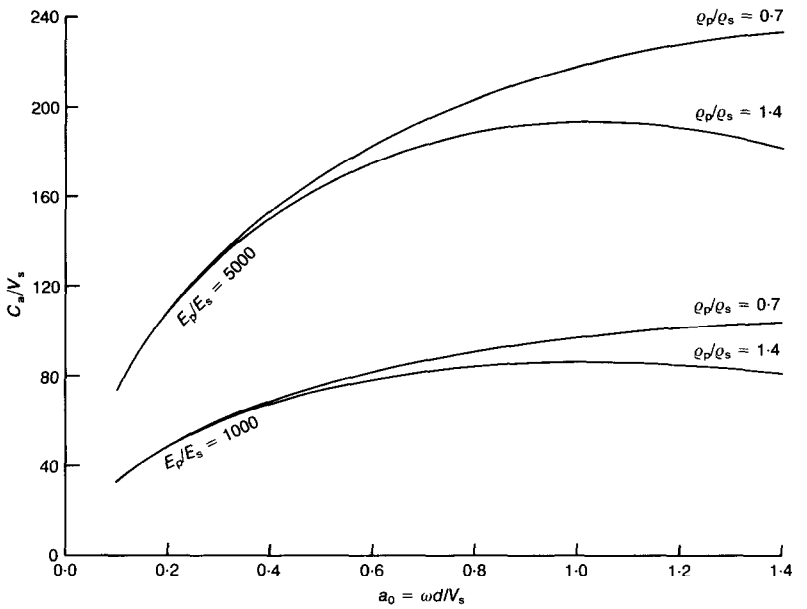

Fig. 3. Dispersion relationships for phase velocity of waves in an axially vibrating infinitely long pile, in the frequency range of greatest interest, for two values of pile-to-soil Young's moduli ratio and two values of pile-to-soil mass densities ratio

$a_0 < 0{\cdot}8$), the ratio C_a/V_s attains relatively high values, of the order of 70 for $E_p/E_s = 1000$ and 170 for $E_p/E_s = 5000$. As a result, phase differences introduced by waves travelling down the pile would be negligible compared with the phase differences due to S-waves travelling in the soil from one pile to another. Thus, for example, with a pile of $L = 20d$ and $\rho_p = 1{\cdot}4\rho_s$, the error yielded by assuming synchronous wave emission would be of the order of 4% (for $E_p/E_s = 1000$) and 2% (for $E_p/E_s = 5000$).

To show this more clearly, the phase angle from equation (16) is

$$\phi(z) = \omega t - Rz \sin \frac{\theta}{2} \tag{25}$$

Figure 4 shows the phase differences $\Delta\phi = \Delta\phi(z)$ between the displacement of a section at depth z and that at the head of the pile, for two values of α_0 (0·2 and 0·5) and for three values of E_p/E_s: 5000 (typical for soft soil), 1000 (medium–stiff soil), and 300 (stiff–hard soil). Evidently, even in the case of hard soil (i.e. in the case of a relatively very flexible pile), the pile at a depth $z = 20d$ has a phase difference with the head of only about 15°. For the softer soil (stiffer pile), $\Delta\phi \leqslant 4°$. These differences are indeed insignificant (within engineering accuracy), and therefore the assumption of synchronous emission is a reasonable approximation. A similar conclusion can be drawn from Fig. 3 of Novak (1977).

As these results were derived on the basis of an infinitely long bar on dynamic Winkler foundation model, it is of interest to show their general validity for piles of finite length supported by a visco-elastic continuum. To this end, a rigorous finite element study was conducted for a pile of slenderness ratio $L/d = 20$ embedded in a deep homogeneous stratum and having $E_p/E_s = 1000$ or 5000. Fig. 5 shows the distribution along the length of the pile of the real and imaginary parts of the vertical pile displacement, $v = v(z)$, for the same two values (0·2 and 0·5) of the frequency factor a_0. Evidently, the imaginary and real components of the displacement as well as the resulting phase angle remain almost constant with depth; hence, the phase differences between various points along the pile and its head (also plotted in Fig. 5) are very small, and their values are very close to those predicted by the analytical method (Fig. 4). Thus, the analytical results and the hypothesis of synchronous wave emission are largely substantiated. However, in much stiffer soils, for which the moduli ratio E_p/E_s may attain values lower than, say, 300 (e.g. hollow pipe piles in hard soil), the apparent phase velocity C_a becomes a smaller multiple of V_s, and then for very slender piles ($L > 40$) phase differences along the pile may reach 40° at higher frequencies. In

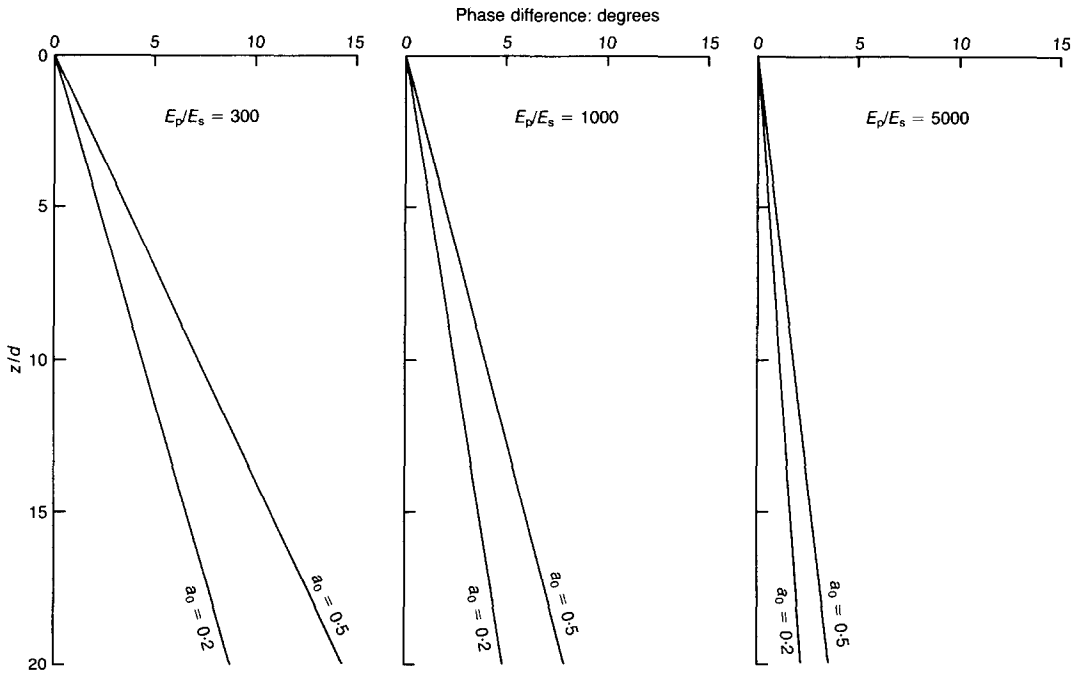

Fig. 4. Phase difference between displacements at depth z and at pile top for two values of the frequency factor

such cases the assumption of synchronous emission might not be applicable. Dobry & Gazetas (1988) have reported that their simple pile group interaction factor (equation (1)), leads to an overprediction of pile group effects for values of E_p/E_s lower than 300.

A further observation can be made on the dispersion relation of equation (19). While Fig. 3 plots C_a for a homogeneous halfspace, in reality, bedrock or at least a stiff rock-like soil layer is likely to exist at some depth below the ground surface. Then the soil deposit is a deep stratum rather than a true halfspace, although a long pile can still be modelled as an infinitely long beam. Below the stratum cutoff frequency ω_c the pile–soil system radiates very little energy, and c_z essentially reflects only the hysteretic material damping in the soil. Without material damping $c_z = 0$, and the solution reduces to the case discussed by Wolf (1985, 1988), in which the phase velocity is indeed infinite (as $\theta = 0$). Therefore as a first approximation, for $\omega < \omega_c$: $C_a \to \infty$. In general, however, the phase velocity is finite provided that a mechanism of energy dissipation exists along the pile (radiation or material damping).

It is also of interest to study the complete evolution of the phase wave velocity over an extreme range of frequencies ($0 < a_0 < 10$), as shown in Fig. 6 for a pile with $E_p/E_s = 1000$ and in Fig. 7 for a pile with $E_p/E_s = 5000$ for two different pile mass densities: $\rho_p = 1{\cdot}4\rho_s$ and $0{\cdot}7\rho_s$. The solid curve represents the developed dispersion relation; it is obvious that equations (19) and (22) give the same value for both C_a and dC_a/da_0 at the characteristic frequency $\bar{\omega}_z$. Also plotted in Figs 6 and 7 are the dispersion relations of two simpler associated systems, namely a semi-infinite rod on elastic–Winkler foundation and a semi-infinite unsupported rod. These two systems have been studied extensively in the wave-propagation literature (e.g. Graff, 1975; Achenbach, 1976), and are obviously particular cases of the pile system studied here (Fig. 2). The phase velocity C_E for the rod on elastic foundation is obtained from equations (19) and (22) by setting $c_z = 0$ at all frequencies. As discussed by Wolf (1985) and mentioned above, C_E becomes infinite at and below the characteristic frequency $\bar{\omega}_z$. Therefore

$$C_E = \infty, \quad \text{if } \omega \leqslant \bar{\omega}_z \tag{26a}$$

$$C_E = V_s \frac{a_0}{2} \left(\frac{s_2 \pi}{(\pi/4) s_1 s_3 a_0^2 - f_1} \right)^{1/2}, \quad \text{if } \omega > \bar{\omega}_z \tag{26b}$$

The phase velocity C_L for longitudinal waves in an unsupported rod (called bar or rod wave

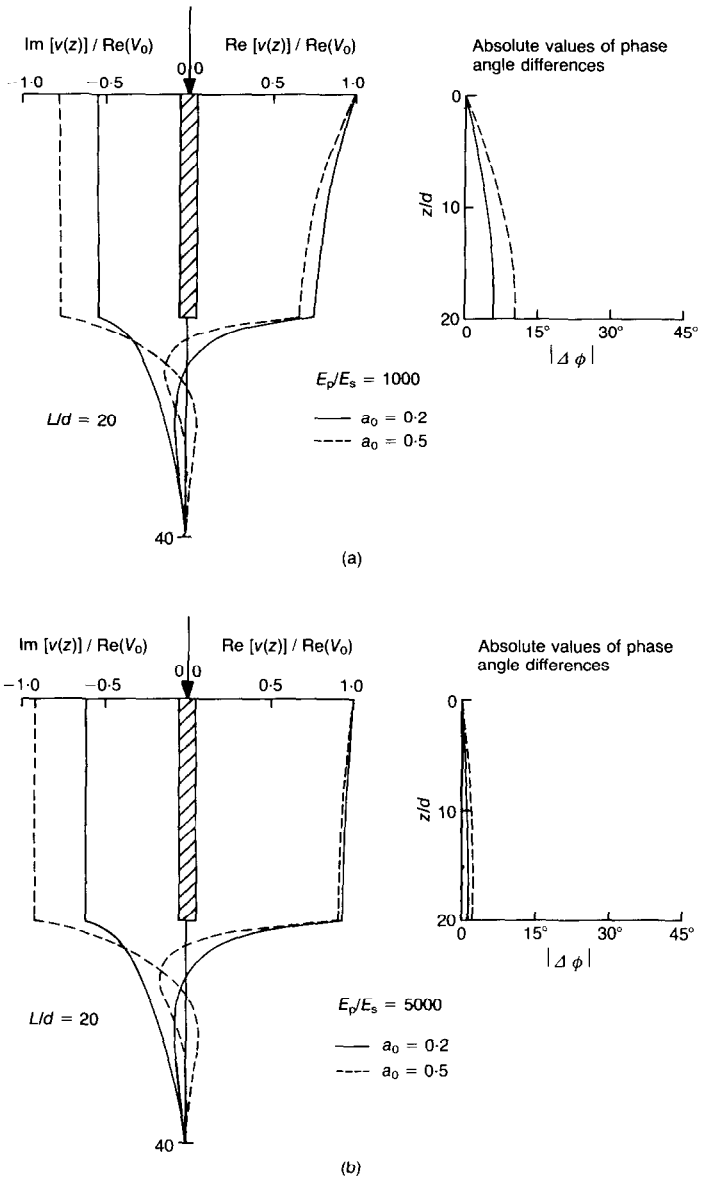

Fig. 5. Distribution with depth of normalized vertical pile displacements and pile–displacement phase differences for an $L/d = 20$ pile in a deep homogeneous soil: (a) $E_p/E_s = 1000$; (b) $E_p/E_s = 5000$; displacements of soil below the pile are also plotted; real part denotes the component of displacement that is in phase with the applied force and imaginary part denotes the component of displacement that is out of phase with the applied force; results were obtained with a dynamic finite element formulation (Blaney *et al.*, 1976) for the two shown values of the frequency factor

velocity) is equal to $\sqrt{(E_p/\rho_p)}$ only when lateral inertia effects are ignored. However, for the frequency range studied ($a_0 < 10$), the decline of C_L with frequency (called the Pochhammer effect in wave theory (Graff, 1975)) is indistinguishable in the scale of the figure.

Figures 6 and 7 reveal an interesting feature: all three phase wave velocities C_a, C_E and C_L

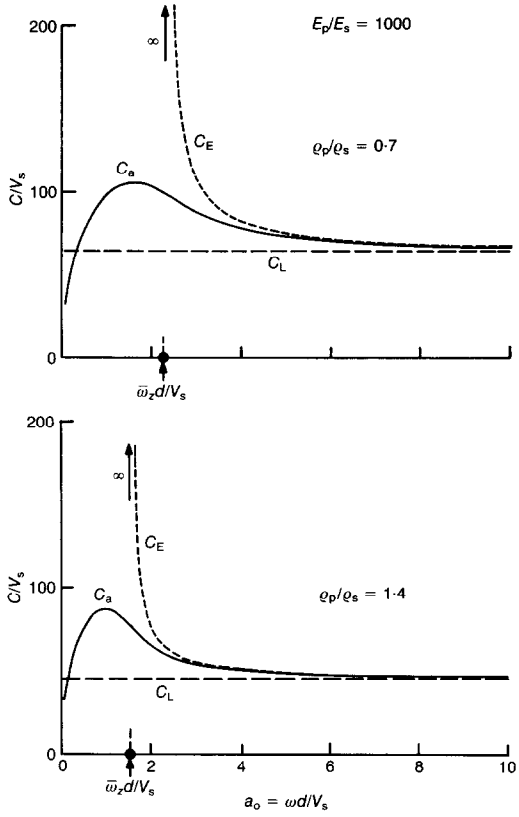

Fig. 6. Comparison of dispersion relations for three longitudinal phase velocities: C_a, for a pile supported on axial springs and dashpots (modelling embedment in halfspace); C_E, for a bar on axial springs; C_L for an unsupported bar—two different values of pile-to-soil mass densities ratio; E_p/E_s = 1000

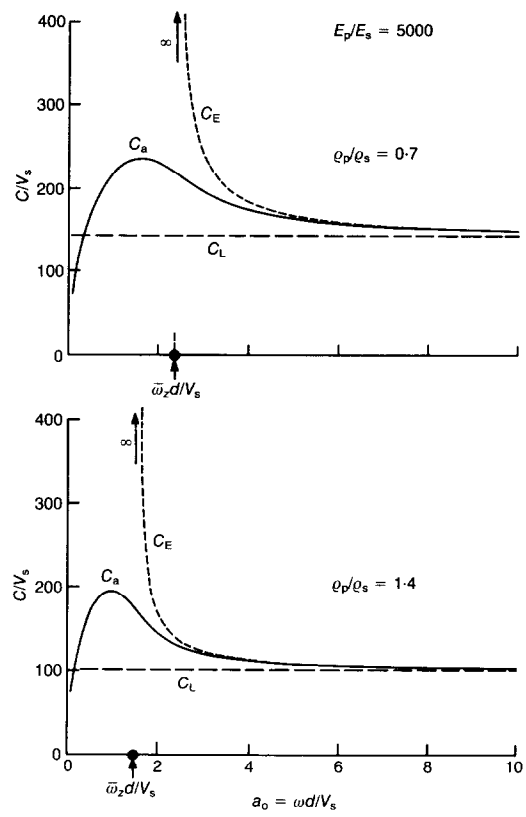

Fig. 7. Comparison of dispersion relations for three longitudinal phase velocities: C_a, for a pile supported on axial springs and dashpots (modelling embedment in halfspace); C_E, for a bar on axial springs; C_L for an unsupported bar—two different values of pile-to-soil mass densities ratio; E_p/E_s = 5000

reach identical asymptotic values at high frequencies. It appears that at these frequencies pile inertia effects dominate, while the resistance of the supporting springs and dashpots becomes negligibly small in comparison.

LATERAL VIBRATION

Governing equation and solution

With regard to lateral excitation, the assumption of an infinitely long pile is quite appropriate even for stiff piles, as their active length is usually smaller than the total pile length. Indeed, for a pile on Winkler foundation, the active length below which the pile deformations are negligible is given by Randolph (1981) as

$$l_c \approx 4\left(\frac{E_p I}{k_x}\right)^{1/4} \approx 1{\cdot}75d\left(\frac{E_p}{E_s}\right)^{1/4} \qquad (27)$$

where the expression for k_x from equation (2c) has been used. For the typical values of E_p/E_s = 1000 and 5000, the active lengths from equation (27) are only about $10d$ and $15d$ respectively. As shown by Krishnan *et al.* (1983) and Gazetas & Dobry (1984a, 1984b) the concept of the active length is also valid under dynamic harmonic loading, although the exact values of l_c are slightly larger than those predicted from equation (27). Hence, in most cases, piles respond as infinitely long beams.

The pile is modelled as an Euler–Bernoulli beam, where the effects of rotatory inertia and shear distortion are ignored. The deflected state of the pile and the forces acting on an element are shown in Fig. 2, with $u(z, t)$ denoting the horizontal displacement at depth z and time t. Zero slope is imposed at pile head to account for the shape of deformation induced by a horizontally-translating rigid pile cap (fixed-head pile, in

geotechnical terminology). For a harmonic steady-state excitation $u(z, t) = u(z) \exp(i\omega t)$, dynamic equilibrium gives

$$E_p I_p \frac{d^4 u(z)}{dz^4} + (k_x + i\omega c_x - m\omega^2)u(z) = 0 \quad (28)$$

The solution to equation (28) is sought separately for the two cases of $\omega < \bar{\omega}_x$ and $\omega \geqslant \bar{\omega}_x$, where $\bar{\omega}_x = (k_x/m)^{1/2}$.

First, consider $\omega < \bar{\omega}_x$. This is again the usual range of greatest interest in foundation dynamics, corresponding approximately to $a_0 < 1{\cdot}8$. The solution of equation (28) derived in Appendix 1 takes the form

$$u(z, t) = \frac{U_0}{2}\{(1 + i) \exp(-Rbz) \times \exp[i(\omega t - Raz)] + (1 - i) \exp(-Raz) \times \exp[i(\omega t + Rbz)]\} \quad (29)$$

where $U_0 = u(0)$ is the displacement amplitude at the pile head and R, θ, a and b are as given in Appendix 1.

For an applied harmonic load $P_0 \exp(i\omega t)$ with P_0 real, U_0 is complex

$$U_0 = \frac{P_0(\gamma_1 - i\gamma_2)}{E_p I_p R^3(\gamma_1^2 + \gamma_2^2)} \quad (30)$$

where

$$\gamma_1 = -a^3 - b^3 + 3a^2 b + 3ab^2 \quad (31a)$$

$$\gamma_2 = a^3 - b^3 + 3a^2 b - 3ab^2 \quad (31b)$$

and a, b are as given in Appendix 1. It can be checked that when $\omega = 0$ (i.e. under static loading), $a = b = 1$, $\gamma_1 = 4$ and $\gamma_2 = 0$; then equation (30) reduces to the familiar static expression

$$U_0 = \frac{P_0}{4E_p I_p \lambda^3} \quad (32)$$

with λ (from Appendix 1) being simply equal to the static value (Elson, 1984)

$$\lambda = (k_x/4E_p I_p)^{1/4} \quad (33)$$

The first term in the parentheses in equation (29) corresponds to a downwardly propagating wave and the second term to an upwardly propagating wave, both with amplitude decaying exponentially as with z. It should be emphasized that the two waves coexist and the displacement distribution along the pile should always be regarded as the superposition of both. Nevertheless, the phase velocity of each wave separately can be identified, giving a dual dispersion relation

$$C_a^{\downarrow} = \frac{\omega}{R\left(\cos\frac{\theta}{4} + \sin\frac{\theta}{4}\right)} \quad (34a)$$

$$C_a^{\uparrow} = \frac{\omega}{R\left(\cos\frac{\theta}{4} - \sin\frac{\theta}{4}\right)} \quad (34b)$$

Second, consider $\omega \geqslant \omega_x$, which translates approximately to $a_0 > 1{\cdot}8$, a frequency range of less practical interest, which is examined here as providing insight into asymptotic behaviour at high frequencies. Following a similar procedure to the one already outlined, gives the solution

$$u(z, t) = \frac{U_0}{2}\{(1 + i) \exp(-Rqz) \exp[i(\omega t - Rpz)] + (1 - i) \exp(-Rpz) \exp[i(\omega t + Rqz)]\} \quad (35)$$

where

$$R = \left[\frac{(m\omega^2 - k_x)^2 + (\omega c_x)^2}{(E_p I_p)^2}\right]^{1/8} \quad (36)$$

$$p = \cos\frac{\theta}{4} > 0, \quad q = -\sin\frac{\theta}{4} > 0 \quad (37)$$

and θ is given by the same expression as for the case $\omega < \bar{\omega}_x$ (given in Appendix 1), but now takes a negative value ($-\pi/2 < \theta < 0$). Again, the solution is a superposition of two waves, one propagating downwards and one propagating upwards, with respective phase velocities

$$C_a^{\downarrow} = \frac{\omega}{R\cos\frac{\theta}{4}} \quad (38a)$$

$$C_a^{\uparrow} = \frac{\omega}{-R\sin\frac{\theta}{4}} \quad (38b)$$

In the completely hypothetical case of $c_x = 0$, one would have $\theta = 0$, $p = 1$, $q = 0$, $R = (m\omega^2 - k_x/E_p I)^{1/4} = \lambda$; and equation (36) would reduce to

$$u(z, t) = \frac{U_0}{2} = \{(1 - i) \exp(-\lambda z) \exp(i\omega t) + (1 + i) \exp[i(\omega t - \lambda z)]\} \quad (39)$$

In this case only down-going waves exist, as the term corresponding to incoming waves reduces to a decaying exponential.

DISCUSSION

From equations (34) and (38), the phase velocities $C_a^{\downarrow}$ and $C_a^{\uparrow}$ of the direct (down-going) and reflected (up-coming) waves are shown as solid lines in Figs 8 and 9, over a wide range of the frequency factor $0 < a_0 < 10$. Also plotted in Figs 8 and 9 are the frequency-dependent phase velocities of a semi-infinite beam on the elastic–Winkler foundation (C_W), and a semi-infinite unsupported flexural beam C_F. These two cases are recovered from the developed formulation for $c_x = 0$ and $k_x = c_x = 0$, respectively. The corresponding phase velocities are

$$C_W = \infty, \quad \text{if } \omega < \bar{\omega}_x \tag{40a}$$

$$C_W = V_s \frac{a_0}{2}\left(\frac{s_2 \dfrac{\pi}{4}}{\dfrac{\pi}{4} s_1 s_3 a_0^2 - f_1}\right)^{1/4}, \quad \text{if } \omega \geq \bar{\omega}_x \tag{40b}$$

$$C_F = V_s \frac{\sqrt{a_0}}{2}\left(\frac{s_2}{s_1 s_3}\right)^{1/4} \tag{41}$$

where $f_1 = 1{\cdot}2$ and $f_2 = 6 s_1 a_0^{3/4} + 2\beta f_1$.

The following trends are worthy of note.

The presence of material and geometric damping in the pile–soil system has a highly significant effect on the nature of propagating waves and the phase velocities. As mentioned above, an upward propagating (reflected) wave is generated only in the damped system. Moreover, at the low frequency range of usual interest ($a_0 < 1$), while the phase velocity becomes infinite in the undamped case C_W, both $C_a^{\downarrow}$ and $C_a^{\uparrow}$ achieve very small values and, in fact, tend to zero with decreasing frequency. Hence the presence of a rigid soil layer or rock at a shallow depth that would create a cutoff frequency ω_s, below which

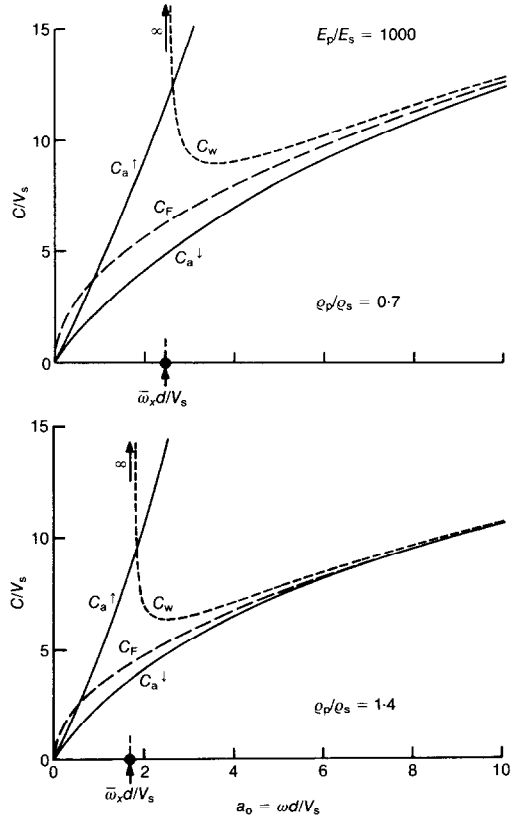

Fig. 8. Phase wave velocities of beams in lateral harmonic oscillations; the two solid lines are for the up-going and down-going waves in a pile on lateral springs and dashpots (modelling embedment in halfspace); C_W is for a flexural beam on lateral springs; C_F is for an unsupported flexural beam—two different values of pile-to-soil mass densities ratio; $E_p/E_s = 1000$

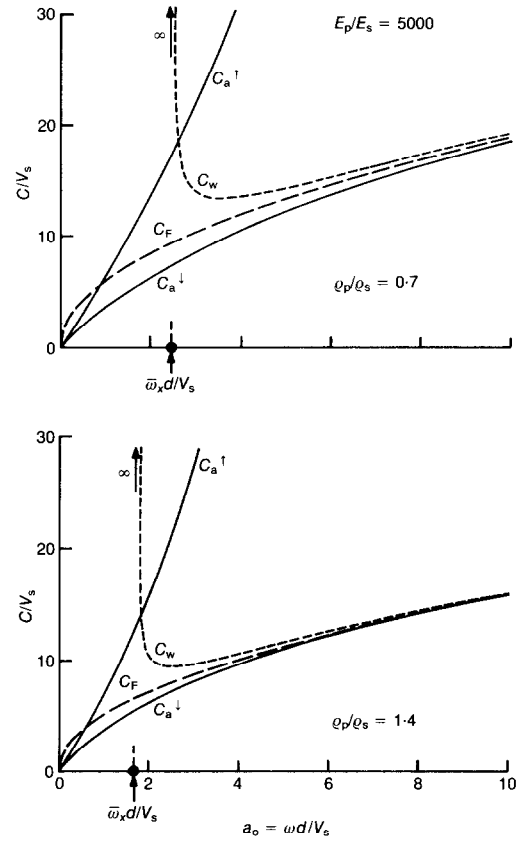

Fig. 9. Phase wave velocities of beams in lateral harmonic oscillations: the two solid lines are for the up-going and down-going waves in a pile on lateral springs and dashpots (modelling embedment in halfspace); C_W is for a flexural beam on lateral 'springs'; C_F is for an unsupported flexural beam—two different values of pile-to-soil mass densities ratio; $E_p/E_s = 5000$

radiation damping diminishes, deserves attention. In such a case, if soil and pile material damping are ignored, then $c_x = 0$, $\theta = 0$, $a = b = 1$, $R = (k_x - m\omega^2/4E_p I_p)^{1/4} = \lambda$ (real number), and equation (29) simplifies to

$$u(z, t) = U_0 \, e^{-\lambda z}(\sin \lambda z + \cos \lambda z) \, e^{i\omega t} \qquad (42)$$

which describes a standing wave and is identical in form to the static solution (Scott, 1981), to which it reduces for $\omega = 0$. Hence, in this case there are no propagating waves (infinite apparent phase velocity) and all points move in phase, although with an amplitude decreasing exponentially with depth, in accordance with the behaviour of the elastically restrained beam (equation (42)) already described.

The phase velocity $C_a^{\downarrow}$ of the downwardly propagating wave in the pile remains very close to the velocity C_F of the (unsupported) flexural beam for all but the very low frequencies. Nevertheless, it is perhaps surprising that $C_a^{\downarrow}$ is much closer to C_F than to C_W. Hence, neglecting radiation and material damping may adversely affect even the nature of the solution.

The phase velocities of the three downwardly propagating waves, namely $C_a^{\downarrow}$ in the pile, C_W in the elastically-restrained beam and C_F in the flexural beam, converge to a single curve at high frequencies (say $a_0 > 3$), and tend to infinity by growing in proportion to $\sqrt{\omega}$. However, the velocity $C_a^{\uparrow}$ of the reflected wave in the pile soon diverges significantly and tends to infinity as a power of ω. That the phase velocities grow without limit with increasing frequency is an inaccuracy attributed to neglecting rotatory inertia and shear distortion effects. Such effects must be included in the formulation if more correct values are to be obtained for phase velocities at very high frequencies.

No clear conclusions can be drawn from Figs 8 and 9 regarding the assumption of synchronous wave emission from a laterally oscillating pile. Both $C_a^{\downarrow}$ and $C_a^{\uparrow}$ attain relatively small values, of about 2–5 V_s, in the frequency range of greatest interest, even for a relatively stiff pile ($E_p/E_s = 5000$). It seems that the only way to assess the significance of such wave velocities is to examine the phase differences among lateral displacements along the pile.

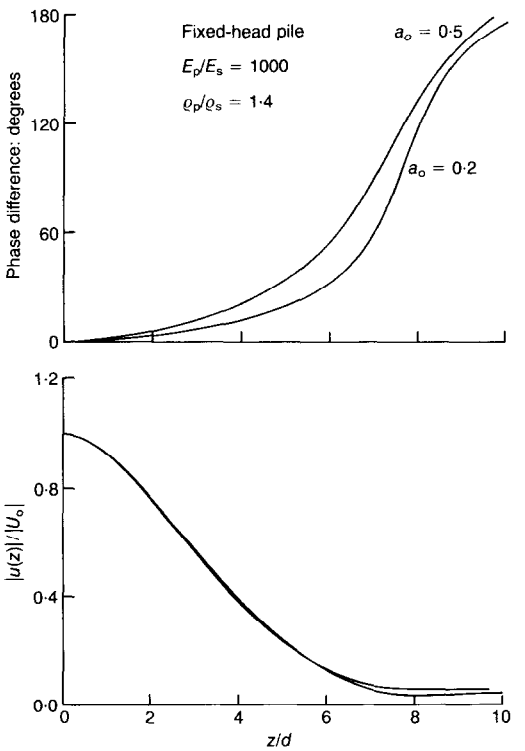

Fig. 10. Variation with depth of phase differences and normalized lateral deflexion amplitudes at two frequency factors

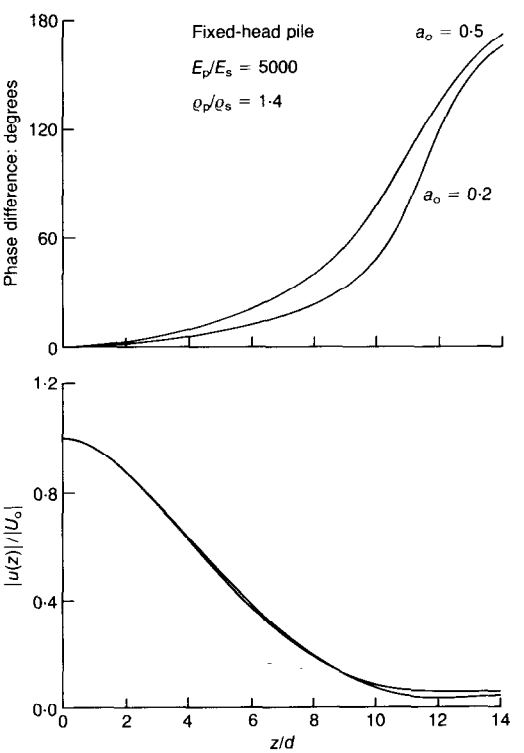

Fig. 11. Variation with depth of phase differences and normalized lateral deflexion amplitudes at two frequency factors

To this end, the phase of the motion at a particular depth z in time t is computed from

$$\phi(z, t) = \tan^{-1}\left\{\frac{\text{Im}\,[u(z, t)]}{\text{Re}\,[u(z, t)]}\right\} \tag{43}$$

and for z equal to zero the phase becomes

$$\phi(0, t) = \tan^{-1}\left\{\frac{\text{Im}\,[u(0, t)]}{\text{Re}\,[u(0, t)]}\right\} = \omega t \tag{44}$$

The phase difference between the motion at depth z and the motion at the head of the pile

$$\Delta\phi = \omega t - \phi(z, t) \tag{45}$$

is plotted in Figs 10 and 11 as a function of z/d for two values of the dimensionless frequency a_0 (0·2 and 0·5) for $E_p/E_s = 1000$ and 5000. It is clear that phase differences remain quite small up to a certain depth, beyond which they increase rapidly, especially at higher frequencies. Figs 10 and 11 also show the normalized amplitude of pile displacements plotted against z/d. It is evident that, strictly speaking, the assumption of simultaneous emission is not valid. Nevertheless, it is also clear that phase differences become substantial only at relatively large depths where the displacement amplitude has decreased significantly; thus waves emitted from such depths would have a negligible amplitude and their phase differences would be of little, if any, consequence to adjacent piles. Hence, the error introduced by assuming synchronous wave emission along the pile would in most cases be acceptable. This may explain the successful performance of the method developed by Dobry & Gazetas (1988), Makris & Gazetas (1992), and Gazetas & Makris (1991), as shown in Fig. 1.

CONCLUSIONS

Axial vibrations

When an infinitely long pile embedded in a realistic dynamic–Winkler model of a homogeneous halfspace is subjected to axial harmonic head loading, it undergoes steady-state oscillations due to a compression–extension wave that propagates downwards with amplitude decaying exponentially with depth, and a frequency-dependent phase velocity C_a (dispersive system).

In the frequency range of greatest interest in foundation dynamics ($0{\cdot}2 \leqslant a_0 \leqslant 0{\cdot}8$), C_a initially increases with frequency and for typical real-life piles achieves quite large values compared to the S-wave velocity in soil V_s. As a result, phase differences between displacements along the oscillating pile are very small and can be neglected in approximate studies of through-soil interaction between two adjacent piles—a conclusion for which additional (direct and indirect) supporting evidence is provided in this Paper.

In the frequency range of interest considered, the wave velocity C_E of a bar elastically restrained solely by Winkler springs is infinite. However, C_a could approach infinity only at frequencies below a possible stratum cutoff frequency (when radiation damping vanishes) if all material hysteretic damping were ignored.

At high frequencies ($a_0 \approx 5$–10), C_a, C_E and the (unsupported) bar wave velocity C_L reach the same asymptotic value, equal to about $\sqrt{(E_p/\rho_p)}$ (lateral inertia Pochhammer effects are not as yet discernible).

Lateral vibrations

During lateral steady-state oscillation under harmonic fixed-head horizontal leading, two waves develop in the pile: a downwardly propagating (direct) wave with phase velocity $C_a^{\downarrow}$, and an upwardly propagating (reflected) wave with different phase velocity $C_a^{\uparrow}$—both having amplitude decaying exponentially with depth.

The two phase velocities $C_a^{\downarrow}$ and $C_a^{\uparrow}$ increase monotonically with frequency, the latter at a much faster rate. In the frequency range of greatest interest they both attain very low values, only a few times larger than V_s in the soil but smaller than C_F (the phase velocity of an unsupported flexural beam).

In contrast to the spring-and-dashpot supported pile, only one downwardly propagating wave develops in a beam supported solely on springs. Moreover, the phase velocity C_W in the latter is infinitely large below the characteristic frequency $\bar{\omega}_x = \sqrt{(k_x/m)}$, i.e. in the frequency range of greatest interest. Therefore, ignoring the material and especially the radiation damping generated by the soil–pile system would change the nature of the wave propagation in laterally oscillating piles.

Despite the relatively low values of $C_a^{\downarrow}$ and $C_a^{\uparrow}$ at $0 < a_0 < 1{\cdot}8$, the two waves (direct and reflected) combine in such a way that phase differences between pile deflexions at various depths remain quite small along the upper, most active, part of the pile. Such differences increase considerably at greater depths, but this has only a minor effect on how wave energy is radiated from a pile: this observation is significant in the behaviour of pile groups. An exception to this behaviour, however, must be noted: with hollow pipe piles in hard soils, for which $E_p/E_s < 300$, phase differences may become appreciable and the assumption of synchronous emission might lead to a slight overprediction of pile to pile interaction factors.

The phase velocities of the three downwardly propagating waves C_a, C_W and C_F converge to a single curve at high frequencies ($a_0 > 3$), while growing in proportion to $\sqrt{\omega}$.

The results presented may lead to an improved understanding of wave propagation phenomena in piles, and find applications in geotechnical problems involving pile dynamics.

APPENDIX 1. SOLUTION OF EQUATION (28) FOR $\omega < \tilde{\omega}_x$

To obtain the solution of equation (28), first substitute

$$4\lambda^4 = \frac{k_x + i\omega c_x - m\omega^2}{E_p I_p} \tag{46}$$

and then apply the Laplace transform (to accommodate the boundary conditions directly)

$$L\left[\frac{d^4u(z)}{dz^4}\right] + 4\lambda^4 L[u(z)] = 0 \tag{47}$$

Denoting the Laplace transform of $u(z)$ by $\bar{u}(s) = L[u(z)]$ and using standard Laplace transform properties, equation (47) becomes an algebraic equation in the transformed space

$$\bar{u}(s) = u'''(0)\frac{1}{s^4 + 4\lambda^4} + u''(0)\frac{s}{s^4 + 4\lambda^4} + u(0)\frac{s^3}{s^4 + 4\lambda^4} \tag{48}$$

where the prime denotes derivative with respect to z.

Applying the inverse Laplace transform and introducing Euler's complex notation leads to the following solution, with the boundary conditions at $z = 0$ incorporated as unknowns

$$\begin{aligned} u(z) = &-i[\exp(iRaz)\exp(Rbz) - \exp(-iRbz)\exp(Raz)]\left[\frac{u'''(0)}{16\lambda^3} + \frac{u''(0)}{8\lambda^2}\right] \\ &- i[\exp(iRbz)\exp(-Raz) - \exp(-iRaz)\exp(Rbz)]\left[\frac{u'''(0)}{16\lambda^3} - \frac{u''(0)}{8\lambda^2}\right] \\ &+ [\exp(iRaz)\exp(Rbz) + \exp(-iRbz)\exp(Raz)]\left[-\frac{u'''(0)}{16\lambda^3} + \frac{u(0)}{4}\right] \\ &+ [\exp(iRbz)\exp(-Raz) - \exp(-iRaz)\exp(-Rbz)]\left[\frac{u'''(0)}{16\lambda^3} + \frac{u(0)}{4}\right] \end{aligned} \tag{49}$$

To ensure a finite displacement amplitude as z tends to infinity

$$\frac{u'''(0)}{16\lambda^3} + \frac{u''(0)}{8\lambda^2} = 0 \tag{50a}$$

$$-\frac{u'''(0)}{16\lambda^3} + \frac{u(0)}{4} = 0 \tag{50b}$$

Using these expressions and $\exp(i\omega t)$ leads finally to

$$u(z, t) = \frac{U_0}{2}\{(1 + i)\exp(-iRbz)\exp[i(\omega t - Raz)] + (1 - i)\exp(-Raz)\exp[i(\omega t + Rbz)]\} \tag{51}$$

where

$$R = \left[\frac{(k_x - m\omega^2)^2 + (\omega c_x)^2}{(4E_p I_p)^2}\right]^{1/8} \tag{52}$$

$$\theta = \tan^{-1}\left(\frac{\omega c_x}{k_x - m\omega^2}\right), \quad 0 < \theta < \frac{\pi}{2} \tag{53}$$

$$a = \cos\frac{\theta}{4} + \sin\frac{\theta}{4} > 0, \quad b = \cos\frac{\theta}{4} - \sin\frac{\theta}{4} > 0 \tag{54}$$

NOTATION

- $a_0 = \omega d/V_s$ dimensionless frequency
- A_p cross-sectional area of pile
- c_x distributed dashpot constant per unit pile length for soil reaction against pile lateral motion (equation (2d))
- c_z distributed dashpot constant per unit pile length for soil reaction against pile vertical motion (equation (2b))
- C_a phase velocity of wave propagating in an infinite rod supported by visco-elastic foundation and subjected to axial vibration
- $C_a^{\downarrow}$ phase velocity of down-going wave propagating in an infinite flexural beam supported by visco-elastic foundation and subjected to lateral vibration
- $C_a^{\uparrow}$ phase velocity of up-coming wave propagating in an infinite flexural beam supported by visco-elastic foundation and subjected to lateral vibration
- C_E phase velocity of wave propagating in an infinite rod supported by elastic (Winkler) foundation and subjected to axial vibration
- C_F phase velocity of wave propagating in an infinite unsupported flexural beam subjected to lateral vibration
- C_L phase velocity of wave propagating in an infinite unsupported rod subjected to axial vibration (longitudinal waves)
- C_W phase velocity of wave propagating in an infinite flexural beam supported by elastic (Winkler) foundation and subjected to lateral vibration
- d pile diameter
- E_p, E_s Young's moduli of pile and soil
- i imaginary unit $\sqrt{(-1)}$
- I_p cross-sectional moment of inertia of pile
- k_x distributed spring constant per unit pile length for soil reaction against pile vertical motion (equation (2c))
- k_z distributed spring constant per unit pile length for soil reaction against pile vertical motion (equation (2a))
- m distributed mass per unit length of pile

$P_0 \exp(i\omega t)$ harmonic load at the pile head
r_0 pile radius
s independent variable in Laplace space
S axis-to-axis distance between interacting piles
$u(z, t)$ horizontal pile displacement

$U_0 \exp(i\omega t)$ harmonic displacement of the pile head
$v(z, t)$ vertical pile displacement
$V_0 \exp(i\omega t)$ harmonic vertical displacement of the pile head
V_s S-wave velocity in soil
β damping ratio of the soil
$\Delta\phi$ phase difference between the motion at depth z and the motion at the pile head at a specific time
λ wave number (equation (44) or (47))
ν Poisson's ratio of the soil
$\phi(z, t)$ phase of the pile motion at a particular depth z at time t
ω circular frequency of oscillation
ω_c stratum cutoff frequency in vertical (compression–extension) vibrations
ω_s stratum cutoff frequency in horizontal (shear) vibrations
$\bar{\omega}_x$ characteristic frequency in horizontal (lateral) vibration, $\sqrt{(k_x/m)}$
$\bar{\omega}_z$ characteristic frequency in vertical (axial vibration, $\sqrt{(k_z/m)}$

REFERENCES

Achenbach, J. D. (1976). *Wave propagation in elastic solids.* North-Holland.

Blaney, G. W., Kausel, E. & Roesset, J. M. (1976). Dynamic stiffness of piles. *Proc. 2nd Int. Conf. Numer. Meth. Geomechan.* Blacksburg **2,** 1001–1012.

Dobry, R. & Gazetas, G. (1988). Simple method for dynamic stiffness and damping of floating pile groups. *Géotechnique* **38,** No. 4, 557–574.

Dobry, R., Vicente, E., O'Rourke, M. J. & Roesset, J. M. (1982). Horizontal stiffness and damping of single piles. *J. Geotech. Engng Am. Soc. Civ. Engrs* **108,** GT3, 439–459.

Elson, W. K. (1984). *Design of laterally loaded piles.* Report 103. London: Construction Industry Research Information Association.

Gazetas, G. (1987). Simple physical methods for foundation impedances. *Dynamic behavior of foundations and buried structures.* P. K. Banerjee & R. Butterfield (eds), pp. 45–93. London: Elsevier.

Gazetas, G. & Dobry, R. (1984a). Horizontal response of piles in layered soils. *J. Geotech. Engng Am. Soc. Civ. Engrs* **110,** 20–40.

Gazetas, G. & Dobry, R. (1984b). Single radiation damping model for piles and footings. *J. Engng Mech. Am. Soc. Civ. Engrs* **110,** No. 6, 937–956.

Gazetas, G. & Makris, N. (1991). Dynamic pile–soil–pile interaction I: analysis of axial vibration. *Earthquake Engng Struct. Dyn.* **20,** No. 2, 115–132.

Graff, K. F. (1975). *Wave motion in elastic solids.* Columbus: Ohio State University Press.

Kagawa, T. & Kraft, L. M. (1980). Lateral load–deflection relationship of piles subjected to dynamic loadings. *Soils & Fdns* **20,** No. 4, 19–36.

Kaynia, A. M. & Kausel, E. (1982). *Dynamic stiffness and seismic response of pile groups.* Research Report R82-03. Cambridge, Massachusetts: Massachusetts Institute of Technology.

Krishnan, R., Gazetas, G. & Velez, A. (1983). Static and dynamic lateral deflections of piles in non-homogeneous soil stratum. *Géotechnique* **33,** No. 3, 307–325.

Liou, D. D. & Penzien, J. (1979). Mathematical modelling of piled foundations. *Numerical methods in offshore piling,* pp. 67–74. London: Institution of Civil Engineers.

Makris, N., Gazetas, G. & Fan, K. (1989). Analytical results for pile–soil–pile interaction in vertical harmonic motion. *Proceedings of conference on earthquake resistant construction and design, Berlin,* S. A. Savidis (ed.) Rotterdam: Balkema.

Makris, N. & Gazetas, G. (1992). Dynamic pile–soil–pile interaction II: lateral and seismic response. *Earthquake Engng Struct. Dyn.* **20,** No. 2, 145–162.

Nogami, T. (1983). Dynamic group effect in axial responses of grouped piles. *J. Geotech. Engng Div. Am. Soc. Civ. Engrs* **109,** GT2, 228–243.

Novak, M. (1974). Dynamic stiffness and damping of piles. *Can. Geotech. J.* **11,** No. 4, 574–598.

Novak, M. (1977). Vertical vibration of floating piles. *J. Engng Mech. Div. Am. Soc. Civ. Engrs* **103,** No. 1, 153–168.

Novak, M. (1979). Soil–pile interaction under dynamic loads. *Numerical methods in offshore piling,* pp. 59–74. London: Institution of Civil Engineers.

Novak, M. (1985). Experiments with shallow and deep foundation. *Vibration Problems in Geotechnical Engineering,* G. Gazetas & E. Seling (eds), pp. 1–26. New York: American Society of Civil Engineers.

Novak, M., Nogami, T. & Aboul-Ella, F. (1978). Dynamic soil reaction for plane strain case. *J. Engng Mech. Div. Am. Soc. Civ. Engrs* **104,** No. 4, 1024–1041.

Randolph, M. F. & Wroth, C. P. (1978). Analysis of deformation of vertically loaded piles. *J. Geotech. Engng Div. Am. Soc. Civ. Engrs* **104,** 1465–1488.

Randolph, M. F. & Wroth, C. P. (1979). An analysis of the vertical deformation of pile groups. *Géotechnique* **29,** No. 4, 423–439.

Randolph, M. F. (1981). The response of flexible piles to lateral loading. *Géotechnique* **31,** No. 2, 247–259.

Roesset, J. M. (1984). Dynamic stiffness of pile groups. *Pile foundations,* pp. 263–286. New York: American Society of Civil Engineers.

Roesset, J. M. & Angelides, D. (1980). Dynamic stiffness of piles. *Numerical methods in offshore piling,* pp. 75–82. London: Institution of Civil Engineers.

Scott, R. F. (1981). *Foundation analysis.* London: Prentice-Hall.

Wolf, J. P. (1985). *Dynamic soil-structure interaction.* London: Prentice Hall.

Wolf, J. P. (1988). *Soil–structure interaction in the time-domain.* London: Prentice Hall.

Wolf, J. P. (1992). Cone models for pile foundation. *Piles under dynamic loading,* S. Prakash (ed.), New York: American Society of Civil Engineers.